Journal of Photochemistry and Photobiology A: Chemistry 218 (2011) 1–5

Contents lists available at ScienceDirect

Journal of Photochemistry and Photobiology A: Chemistry

journal homepage: www.elsevier.com/locate/jphotochem

Optical properties of CdS:Mn nanocrystals surface passivated with zinc hydroxide

Wentao Zhang, Hong-Ro Lee*

Department of Applied Materials Engineering, Chungnam National University, Daejeon 305-764, South Korea

ARTICLE INFO

Article history:
Received 13 August 2010
Received in revised form
30 September 2010
Accepted 5 November 2010
Available online 13 November 2010

Keywords:
CdS:Mn
Zinc hydroxide
Surface passivation
Optical property
Nanocrystal

ABSTRACT

For the further application performance, CdS:Mn nanocrystals coated with zinc hydroxide ($Zn(OH)_2$) shells were prepared via wet chemical method. Effect of $Zn(OH)_2$ shells on optical properties of CdS:Mn nanocrystals was investigated. X-ray diffraction (XRD) measurements showed that the CdS nanocrystals have hexagonal wurtzite structure. The morphology and components of CdS:Mn/$Zn(OH)_2$ core/shell nanocrystals were successfully measured by transmission electron microscopy (TEM) with energy-dispersive X-ray (EDX). Luminescence properties (intensity and lifetime) of $^4T_1 \rightarrow {}^6A_1$ transition of Mn^{2+} ions in CdS:Mn/$Zn(OH)_2$ core/shell nanocrystals were significantly enhanced as compared with those of unpassivated CdS:Mn nanocrystals. This expected result was caused by the effective, robust passivation of CdS surface states with $Zn(OH)_2$ shells, which consequently suppressed nonradiative recombination transitions.

© 2010 Elsevier B.V. All rights reserved.

1. Introduction

Due to their unique properties of chemistry and physics, II–VI semiconductor nanocrystals have played an important role in optoelectronic applications as light-emitting diodes and transistors [1–5], biological labels [6,7], and also in photocatalytic applications as radiation source [8–10]. Always, they are used as host materials for rare earth metals and transition metals. Recently, doped II–VI semiconductors (such as ZnS:Cu, CdS:Mn), have been intensively investigated with new luminescence centers [11–13]. The doping ions act as recombination centers for the excited electron–hole pairs and obtain strong and characteristic luminescence. However, with extremely large specific surface area, the surface states of nanocrystals act as luminescent quenching centers and result in serious photodegradation. In addition, experimental results have indicated that any leakage of cadmium from the nanocrystals would be toxic and fatal to a biological system [14,15], and cadmium-containing products are eventually environmentally problematic. Hence, the surface passivation is crucial importance for much wide applications.

In order to achieve well surface passivation and surface protection for core nanocrystals, shell materials with wide band gap, often grown epitaxially on the core surface have to be requested [16]. So inorganically passivated (or core/shell) nanocrystals have been developed and shown dramatically enhanced properties. Comparing with the unpassivated nanocrystals, enhanced photoluminescence (PL) has been observed in CdS/ZnS [17,18], CdS:Mn/ZnS [19,20] core/shell nanophosphors. Depending on the surface passivation, different PL characteristics as a function of UV irradiation have been proposed. In applications, photo-oxidation of ZnS as the nanocrystals surface in the presence of oxygen and water, would led to the formation of $ZnSO_4$ or $Zn(OH)_2$ [21]. This photo-oxidation product is presumably responsible for the enhanced PL emission, serving as a passivation layer on the core surface [22]. Besides, in 1987, Henglein group reported that when a $Cd(OH)_2$ layer was deposited on the CdS nanocrystals [23,24], the luminescence quantum efficiency was increased by 50%, and their luminescence-stability was enhanced by 2000 times.

In this paper, we designed a new core/shell structure with $Zn(OH)_2$ used directly as a passivation layer. Mn-doped CdS nanocrystals were prepared by wet chemical method and then coated on the surface by $Zn(OH)_2$ shells with different thicknesses via precipitation reaction. Comparing with pure CdS:Mn nanocrystals, the impact of $Zn(OH)_2$ shells on luminescent properties of CdS:Mn nanocrystals was investigated.

2. Experimental

2.1. Synthesis of CdS:Mn nanocrystals

CdS:Mn nanocrystals were prepared in aqueous medium as follows. Cadmium acetate (0.02 mol, $Cd(CH_3COO)_2$), manganese acetate (0–0.002 mol, $Mn(CH_3COO)_2$), and appropriate sodium polyphosphate (NaPP) were dissolved in 100 ml distilled water.

* Corresponding author. Tel.: +82 42 821 7636; fax: +82 42 825 5638.
E-mail address: leehr@cnu.ac.kr (H.-R. Lee).

1010-6030/$ – see front matter © 2010 Elsevier B.V. All rights reserved.
doi:10.1016/j.jphotochem.2010.11.005

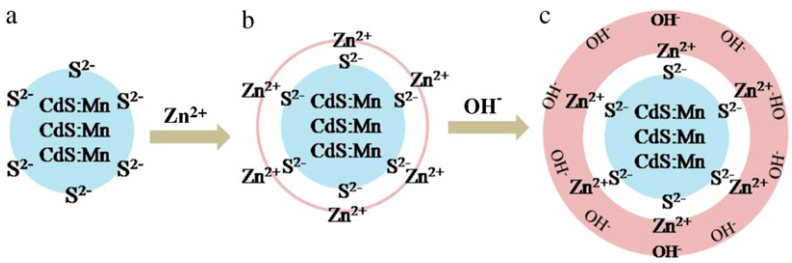

Fig. 1. Formation mechanism of $Zn(OH)_2$ shells on the surface of CdS:Mn nanocrystals. (a) Pure CdS:Mn nanocrystals; (b) Zn^{2+} ions adsorb on the surface of CdS:Mn nanocrystals and (c) OH^- ions approach to the surface of CdS:Mn nanocrystals and react with Zn^{2+} ions to form $Zn(OH)_2$ shells.

Under nitrogen flow, the above mixture was stirred at 60 °C for 30 min. Freshly prepared Na_2S solution was dropwise added to the precursor mixture, and kept strong stirring at 80 °C for 2 h. The molar ratio of S/Cd was chosen more than 1 to ensure that all metal ions were participated in the reaction. After cooled down to room temperature, the final precipitates were separated from solution by centrifugation at 6000 rpm, and then washed with distilled water and anhydrous ethanol several times, respectively. At last, the samples were dried in vacuum at 50 °C for 12 h and collected for further characterization and treatment.

2.2. Synthesis of CdS:Mn/$Zn(OH)_2$ core/shell nanocrystals

In order to make a $Zn(OH)_2$ shell coating on CdS:Mn nanocrystals, the precipitation reaction of $Zn(CH_3COO)_2$ and NaOH was used. Typically, prepared CdS:Mn nanocrystals was put into 100 ml distilled water and ultrasonically dispersed for 1 h, followed by different amount of $Zn(CH_3COO)_2$ aqueous solution was slowly dropped into the CdS:Mn suspension under continuous vigorous stirring. Thirty minutes later, appropriate amount of NaOH dilute solution was added into the suspension to form stoichiometric $Zn(OH)_2$ shell. The thickness of $Zn(OH)_2$ shell was controlled by varying the dosages of $Zn(CH_3COO)_2$ and NaOH (0, 0.25, 0.5, 0.75 and 1 refer to the mole ratios of Zn^{2+} and Cd^{2+} ions). After another 2 h stirring, the resulting precipitates were dealt with as the same as the CdS:Mn nanocrystals.

2.3. Characterization

The as-prepared powder samples were characterized by X-ray diffraction (XRD) on SIEMENS X-ray diffractometer with Cu Kα radiation (λ = 1.5406 Å). The morphology and components of as-obtained products were observed by transmission electron microscopy (TEM) (Hitachi H-800) with an energy-dispersive X-ray (EDX) spectroscope. Photoluminescence measurement was carried out on the absolute ethanol solution in a 1 cm quartz cell at room temperature using 355 nm as the excitation wavelength by a PerkinElmer LS-45 luminescence spectrometer with a spectral resolution of 0.5 nm. Decay curves were measured under sample excitation at 355 nm with a Q-switched Nd–YAG laser (10 ns pulse duration) with a power density at the surface of the sample of about 3 MW cm^{-2} per pulse. The signal was acquired by a Tektronix Digital Store Oscilloscope with a maximum digital storage sampling rate of 20 million samples per second. The rising time of the acquisition system was about 70–80 ns. The samples were mounted in a liquid nitrogen optical dewar (Janis, model VPF-700) equipped with a heater for controlled variation of the sample temperature through a digital temperature controller.

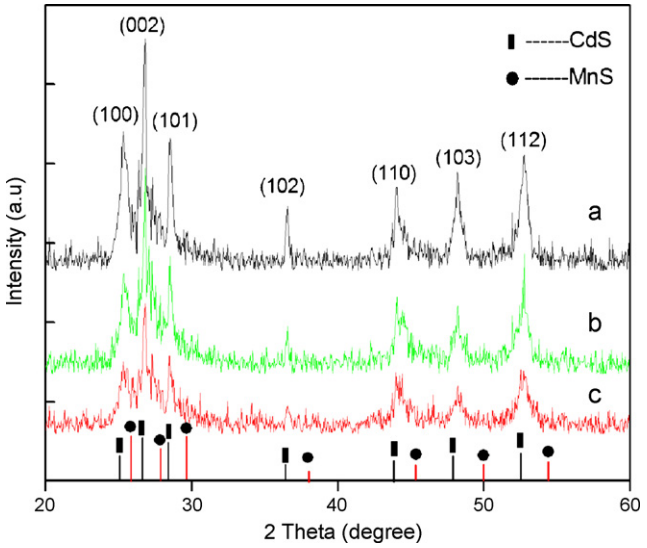

Fig. 2. XRD patterns of CdS:Mn nanocrystals passivated with different $Zn(OH)_2$ thickness: (a) CdS:Mn/$Zn(OH)_2$ (0); (b) CdS:Mn/$Zn(OH)_2$ (0.5) and (c) CdS:Mn/$Zn(OH)_2$ (1). Both the standard CdS and MnS are supplied at the bottom as vertical bars.

3. Results and discussion

3.1. Formation mechanism of $Zn(OH)_2$ shells

The formation mechanism of $Zn(OH)_2$ shells coated on the surface of CdS:Mn nanocrystals can be explained as follows: firstly, because of the molar ratio of reactant ($n_S/n_{Cd} > 1$), many S^{2-} dangling bonds were existed on the surface of CdS:Mn nanocrystals (Fig. 1a). When the $Zn(CH_3COO)_2$ aqueous solution was added into the CdS:Mn suspension, the Zn^{2+} ions (dissociated from $Zn(CH_3COO)_2$) were attracted on the surface of CdS:Mn nanocrystals (Fig. 1b), by existence of the surface S^{2-} dangling bonds. Then, $Zn(OH)_2$ layer was produced on the surface of CdS:Mn nanocrystals as soon as the NaOH aqueous solution was dropped into the suspension, due to the reaction between Zn^{2+} and OH^- ions (dissociated from NaOH), which gradually formed a shell by consuming more Zn^{2+} and OH^- ions (Fig. 1c). At last, CdS:Mn/$Zn(OH)_2$ core/shell nanocrystals were prepared successfully. The thicknesses of shells differ from each other because of the different dosages of $Zn(CH_3COO)_2$ and NaOH.

3.2. Structure and morphology

The crystallinity and phase of CdS:Mn/$Zn(OH)_2$ core/shell nanocrystals were confirmed by XRD analysis. Fig. 2 shows the XRD patterns of CdS:Mn and CdS:Mn/$Zn(OH)_2$ core/shell nanocrystals. The X-ray reflections of CdS:Mn nanocrystals (Fig. 2a) agree

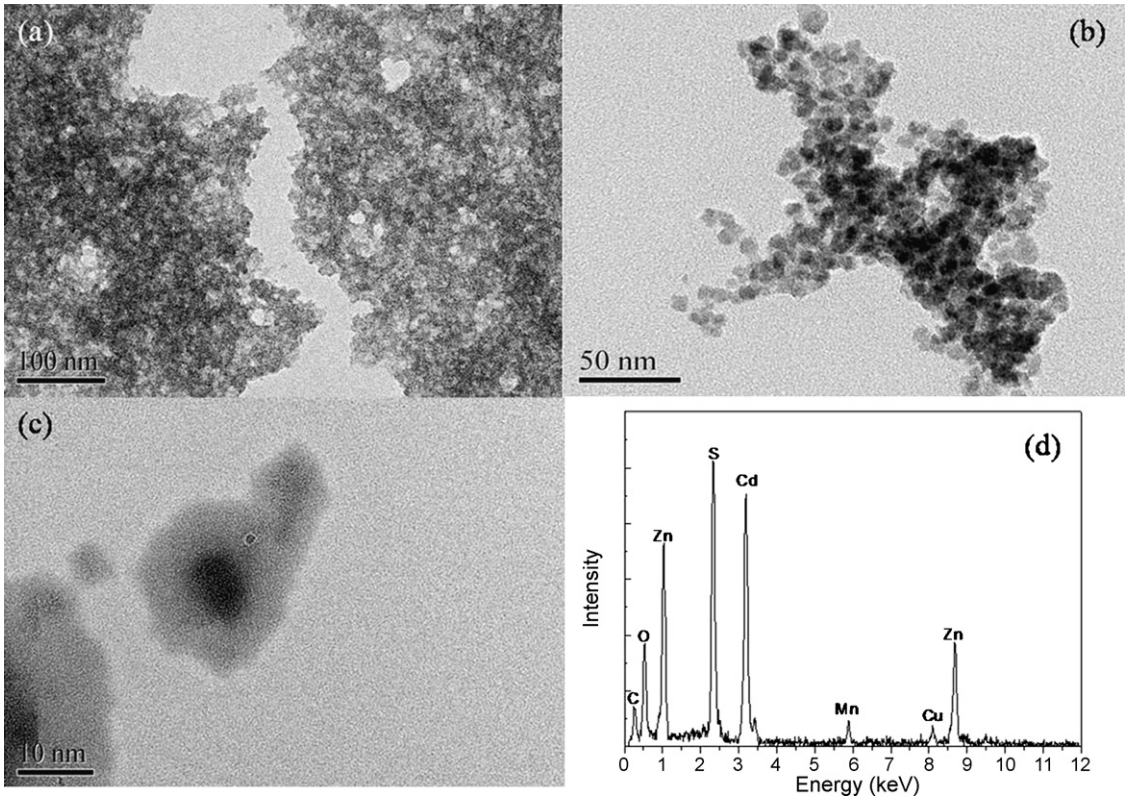

Fig. 3. TEM images of (a) CdS:Mn/Zn(OH)$_2$ (0); (b) CdS:Mn/Zn(OH)$_2$ (0.75); (c) monodispersed CdS:Mn/Zn(OH)$_2$ (0.75) nanocrystals and (d) corresponding EDX spectrum.

with the wurtzite phase of CdS (JCPDS card no. 41-1049). The corresponding peak of MnS phase cannot be observed from the XRD spectra, but all peaks take a little large degree-shift to MnS peak direction because the doped lattices changed weakly comparing with pure CdS crystal. Both these indicate that Mn^{2+} ions have occupied the sites of Cd^{2+} by replacement. After passivated by Zn(OH)$_2$ on the surface of CdS:Mn nanocrystals, XRD peaks of CdS:Mn/Zn(OH)$_2$ (Fig. 2b and c) match with the reflections from the highly crystalline wurtzite CdS. For the patterns of CdS:Mn/Zn(OH)$_2$ nanocrystals, there are no peaks corresponding to Zn(OH)$_2$, because Zn(OH)$_2$ prepared in this way is amorphous [25]. It as well indicates that the crystal structures of ZnS:Mn nanocrystals have not been altered in coating processes. Only the intensity of CdS:Mn/Zn(OH)$_2$ peaks, comparing with that of uncoated CdS:Mn, become a little weak, this is due to Zn(OH)$_2$ layer coating effect.

Fig. 3 shows TEM images of CdS:Mn and CdS:Mn/Zn(OH)$_2$ core/shell nanocrystals. From Fig. 3a, it could be observed that uncoated CdS:Mn nanocrystals was clustered together with each other at state of agglomeration, due to their large special surface and unpassivated surface. After coated with Zn(OH)$_2$ shell, in Fig. 3b we can see that the average diameter of nanocrystals increase, and the dispersion of nanocrystals improved obviously with spherical morphology. For detailed investigation of Zn(OH)$_2$ coating on CdS:Mn surface, TEM image and corresponding EDX (Fig. 3c and d) of an independent CdS:Mn/Zn(OH)$_2$ core/shell nanocrystal were obtained. EDX line analysis was taken on a single particle in samples, and then the corresponding EDX result was got. From Fig. 3d, all elements of CdS:Mn/Zn(OH)$_2$ were observed, except the element of hydrogen. This result proved that the Zn(OH)$_2$ shell was successfully coated on the surface of CdS:Mn nanocrystals. And the atom ratio of Zn/Cd/Mn/O/S was obtained as 19.4/23.1/0.6/30.2/26.0, keeping into correspondence with the starting materials (theoretical molar ratio). In the EDX spectrum, some additional elements were also appeared, such as carbon and copper, which are originated from the grid substrate.

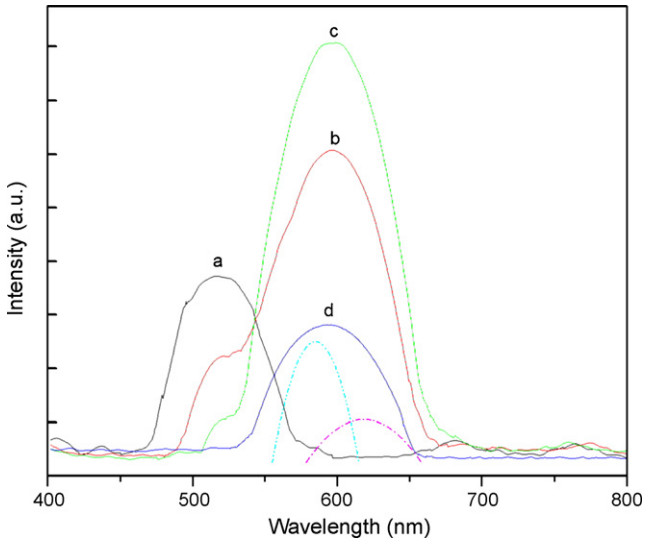

Fig. 4. Luminescence emission spectra excited at 355 nm of (a) CdS nanocrystals and CdS:Mn/Zn(OH)$_2$ (0.5) nanocrystals with various Mn^{2+} concentration; (b) 2 mol%; (c) 5 mol% and (d) 10 mol%. The dash lines at the bottom are Gaussian fitting peaks.

3.3. Photoluminescence properties

Under UV (355 nm) excitation, PL spectra of CdS:Mn/Zn(OH)$_2$ (0.5) nanocrystals with various Mn^{2+} concentration were obtained as shown in Fig. 4. For CdS nanoparticles (Fig. 4a), a green emission band centered at 517 nm could be observed, which was created by the recombination of vacancies inside the lattice. After doped with Mn^{2+} ions, the luminescence centers was transited to Mn^{2+} ions, and the spectra were broadened and the emission wavelength was extended to low energy. For all CdS:Mn nanocrystals, two different emission bands obviously dominated the PL spectra.

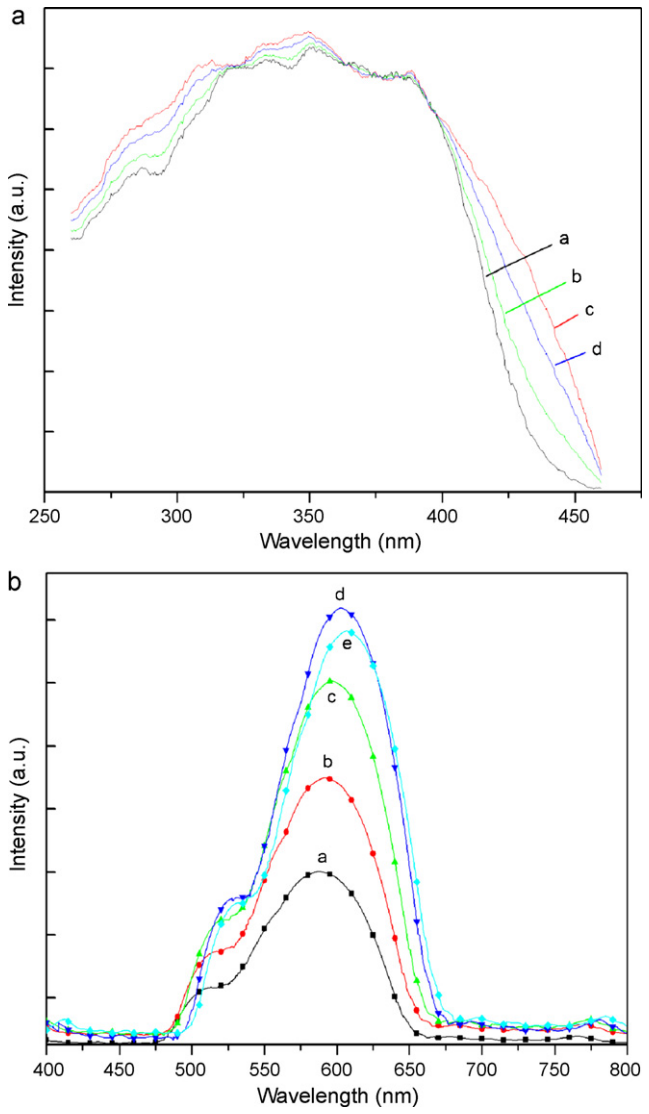

Fig. 5. Excitation spectra (monitored at 595 nm) and emission spectra (excited at 355 nm) of all samples with different $Zn(OH)_2$ shell: (a) CdS:Mn/$Zn(OH)_2$(0); (b) CdS:Mn/$Zn(OH)_2$ (0.25); (c) CdS:Mn/$Zn(OH)_2$ (0.5); (d) CdS:Mn/$Zn(OH)_2$ (0.75) and (e) CdS:Mn/$Zn(OH)_2$ (1).

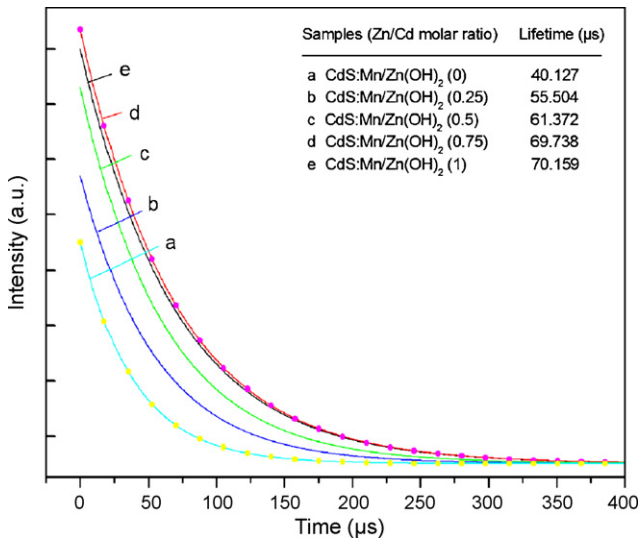

Fig. 6. Luminescence decay curves (monitored at 595 nm) of all samples (a) CdS:Mn/$Zn(OH)_2$ (0); (b) CdS:Mn/$Zn(OH)_2$ (0.25); (c) CdS:Mn/$Zn(OH)_2$ (0.5); (d) CdS:Mn/$Zn(OH)_2$ (0.75) and (e) CdS:Mn/$Zn(OH)_2$ (1) and (•) the corresponding fitting curves.

The first weak emission centered at 510–520 nm was the same as that observed in CdS nanoparticles. The other strong emission that peaked at 590–600 nm originated from the $^4T_1$ to $^6A_1$ transition of Mn^{2+} ions [26]. From the PL spectra of CdS:Mn samples, with the increase of Mn^{2+} concentration, more and more energy was transited to Mn^{2+} centers, accompanying Mn^{2+} emission intensity significantly increased and intrinsic emission of CdS decreased. CdS:Mn nanocrystals reached the highest emission intensity when the concentration of Mn^{2+} increased to 5 mol%. But if the Mn^{2+} content continued to increase, namely, by more than 5 mol%, the Mn^{2+} emission intensity would decrease obviously due to the concentration quenching effect [27].

The PL excitation and emission spectra of 5 mol% Mn doped CdS/$Zn(OH)_2$ core/shell nanocrystals with different $Zn(OH)_2$ thickness (Zn/Cd molar ratio) were shown in Fig. 5. The excitation spectra (Fig. 5a) were checked at emission of 595 nm. In Fig. 5a, the spectra of samples were similar and had strong excitation from 250 to 400 nm, only the intensity of spectra changed a little with different $Zn(OH)_2$ shell. In Fig. 5b, the main emission peak excited at 355 nm with its maximum at about 595 nm was caused by the transition from $^4T_1$ (excited) to $^6A_1$ (ground) of Mn^{2+} ions, indicating that the Mn^{2+} ions had been successfully incorporated into the CdS host lattice. We noticed that with the $Zn(OH)_2$ layer thickening from sample (a) to (e), luminescence of Mn^{2+} centers at 590–607 nm became strong increasingly and had a weak redshift by 17 nm. In uncoated CdS:Mn nanoctystals, some Mn^{2+} ions were averagely distributed in the core, while a large part of Mn^{2+} ions distributed on the surface, which were so near to the quenching center that their luminescence could be quenched easily. Therefore, the luminescence intensity became very weak. Compared with the unpassivated nanocrystals, the PL intensity of the nanocrystals with a core/shell structure was enhanced, which always attributed to the surface passivation effect of the nanocrystals by inhibiting the nonradiative recombination. As luminescence centers, the number of Mn^{2+} ions on the surface gradually reduced with the shell thickening, and this caused the increasing distance from Mn^{2+} ions to the surface of nanocrystals, resulting in the weakening of the energy transfer from Mn^{2+} ions to the quenching center on the surface. But as shown in Fig. 5e, it would lead to the decrease of luminescence intensity that increasing the shell to too thick on the surface.

Luminescent decay curves of CdS:Mn/$Zn(OH)_2$ with different Zn/Cd molar ratio were shown in Fig. 6. Because the Mn^{2+} ions in CdS host were insular luminescent centers, the luminescent decay curves could be fitted with first order exponential function [Eq. (1)]:

$$y = A_1 \times \exp\left(\frac{-x}{t_1}\right) + y_0 \quad (1)$$

where, t_1 is the lifetime of luminescence. The table in Fig. 6 listed the lifetime of the luminescence at 595 nm of each sample. Fig. 6 also exhibited two examples of fitting curves (Fig. 6a and d) by the first exponential function, they were fitted well with original curves. The other three curves were also fitted well. It could be found from that the luminescent lifetime became long increasingly with the thickening of $Zn(OH)_2$ shell. Usually, the surface Mn^{2+} ions act as nonradiative recombination centers and the nonradiative recombination rate is very fast. Once the number of the surface Mn^{2+} ions reduced with $Zn(OH)_2$ passivated shell, the nonradiative transition paths were blocked to some extent, leading to the slowing down of the luminescence decay. These were accord with the results of the emission and excitation spectra.

4. Conclusion

In summary, Mn-doped CdS nanocrystals had been successfully coated with different thick $Zn(OH)_2$ shells. The luminescent properties of CdS:Mn/$Zn(OH)_2$ with different thicknesses of $Zn(OH)_2$ shells and various Mn^{2+} concentration were well studied. With the increasing of Mn^{2+} amount, the luminescence intensity improved, but the concentration quenching effect would play the main role in luminescence intensity when Mn^{2+} concentration exceed 5 mol%. With increasing of the thickness of the $Zn(OH)_2$ shell, the number of surface Mn^{2+} ions decreased and the PL intensity of CdS:Mn/$Zn(OH)_2$ was significantly enhanced. The luminescent decay curves were fitted well with the fitting ones by first order exponential function and the lifetime of the luminescence from Mn^{2+} ions at 590–607 nm was prolonged when the $Zn(OH)_2$ shell thickened. This is caused by the effective, robust passivation of CdS surface states by the $Zn(OH)_2$ shells.

References

[1] R. Xie, U. Kolb, J. Li, T. Basche, A. Mews, Synthesis and characterization of highly luminescent CdSe-core CdS/$Zn_{0.5}Cd_{0.5}$S/ZnS multishell nanocrystals, J. Am. Chem. Soc. 127 (2005) 7480–7488.

[2] M. Amelia, R. Flamini, L. Latterini, Recovery of CdS nanocrystal defects through conjugation with proteins, Langmuir 26 (2010) 10129–10134.

[3] H. Zhao, E.P. Douglas, Preparation of corona-embedded CdS nanoparticles, Chem. Mater. 14 (2002) 1418–1423.

[4] Y. Yang, O. Chen, A. Angerhofer, Y.C. Cao, Radial-position-controlled doping in CdS/ZnS core/shell nanocrystals, J. Am. Chem. Soc. 128 (2006) 12428–12429.

[5] M.A. Zhukovskiy, A.L. Stroyuk, V.V. Shvalagin, N.P. Smirnovaa, O.S. Lytvyn, A.M. Eremenko, Photocatalytic growth of CdS, PbS, and Cu_xS nanoparticles on the nanocrystalline TiO_2 films, J. Photochem. Photobiol. A 203 (2009) 137–144.

[6] H. Yang, P.H. Holloway, S. Santra, Water-soluble silica-overcoated CdS:Mn/ZnS semiconductor quantum dots, J. Chem. Phys. 121 (2004) 7421–7426.

[7] W.C.W. Chan, S. Nie, Quantum dot bioconjugates for ultrasensitive nonisotopic detection, Science 281 (1998) 2016–2018.

[8] J. Das, D. Khushalani, Nonhydrolytic route for synthesis of ZnO and its use as a recyclable photocatalyst, J. Phys. Chem. C 114 (2010) 2544–2550.

[9] Y.-L. Lee, C.-F. Chi, S.-Y. Liau, CdS/CdSe co-sensitized TiO_2 photoelectrode for efficient hydrogen generation in a photoelectrochemical cell, Chem. Mater. 22 (2010) 922–927.

[10] T. Uchihara, M. Shiroma, K. Ishimine, Y. Tamaki, Photoluminescence developed from polystyrene and CdS/polystyrene nanocomposite films in picosecond time range by repetitional irradiation, of excitation femtosecond pulses in PL up conversion measurements, J. Photochem. Photobiol. A 213 (2010) 93–100.

[11] W. Zhang, H.R. Lee, Synthesis and optical property of water-soluble ZnS:Cu quantum dots by use of thioglycolic acid, Appl. Opt. 49 (2010) 2566–2570.

[12] A. Nag, S. Chakraborty, D.D. Sarma, To dope Mn^{2+} in a semiconducting nanocrystal, J. Am. Chem. Soc. 130 (2008) 10605–10611.

[13] A. Nag, S. Sapra, C. Nagamani, A. Sharma, N. Pradhan, S.V. Bhat, D.D. Sarma, A study of Mn^{2+} doping in CdS nanocrystals, Chem. Mater. 19 (2007) 3252–3259.

[14] S.S. Narayanan, S.S. Sinha, P.K. Verma, S.K. Pal, Ultrafast energy transfer from 3-mercaptopropionic acid-capped CdSe/ZnS QDs to dye-labelled DNA, Chem. Phys. Lett. 463 (2008) 160–165.

[15] Y.-P. Sun, X. Wang, F. Lu, L. Cao, M.J. Meziani, P.G. Luo, L. Gu, L.M. Veca, Doped carbon nanoparticles as a new platform for highly photoluminescent dots, J. Phys. Chem. C 112 (2008) 18295–18298.

[16] M. Roskamp, A.K. Schaper, J.H. Wendorff, S. Schlecht, Colloidal CdS/SiO_2 nanocomposite particles from charged colloids of CdS and silica, Eur. J. Inorg. Chem. 2007 (2007) 2496–2499.

[17] D. Chen, F. Zhao, H. Qi, M. Rutherford, X. Peng, Bright and stable purple/blue emitting CdS/ZnS core/shell nanocrystals grown by thermal cycling using a single-source, Chem. Mater. 22 (2010) 1437–1444.

[18] H.-Q. Guo, S.-M. Liu, L. Zhu, Z.-H. Zhang, W. Chen, Z.-G. Wang, Synthesis and luminescence of CdS/ZnS core/shell nanocrystals, Mol. Cryst. Liq. Cryst. 337 (1999) 197–200.

[19] H. Yang, P.H. Holloway, Enhanced photoluminescence from CdS:Mn/ZnS core/shell quantum dots, Appl. Phys. Lett. 82 (2003) 1965–1967.

[20] S. Kar, S. Santra, H. Heinrich, Fabrication of high aspect ratio core–shell CdS–Mn/ZnS nanowires by a two step solvothermal process, J. Phys. Chem. C 112 (2008) 4036–4041.

[21] A.A. Bol, A. Meijerink, Luminescence quantum efficiency of nanocrystalline ZnS:Mn^{2+}. 2. Enhancement by UV irradiation, J. Phys. Chem. B 105 (2001) 10203–10209.

[22] H. Yang, P.H. Holloway, Efficient and photostable ZnS-passivated CdS:Mn luminescent nanocrystals, Adv. Funct. Mater. 14 (2004) 152–156.

[23] L. Spanhel, M. Haase, H. Weller, A. Henglein, Photochemistry of colloidal semiconductors. 20. Surface modification and stability of strong luminescing CdS particles, J. Am. Chem. Soc. 109 (1987) 5649–5655.

[24] Y. Shiraishi, K. Adachi, S. Tanaka, T. Hirai, Effects of poly-N-isopropylacrylamide on fluorescence properties of CdS/$Cd(OH)_2$ nanoparticles in water, J. Photochem. Photobiol. A 205 (2009) 51–56.

[25] H. Zhou, H. Alves, D.M. Hofmann, W. Kriegseis, B.K. Meyer, G. Kaczmarczyk, A. Hoffmann, Behind the weak excitonic emission of ZnO quantum dots: ZnO/$Zn(OH)_2$ core–shell structure, Appl. Phys. Lett. 80 (2002) 210–212.

[26] A. Ishizumi, Y. Kanemitsu, Luminescence spectra and dynamics of Mn-doped CdS core/shell nanocrystals, Adv. Mater. 18 (2006) 1083–1085.

[27] A.A. Bol, A. Meijerink, Luminescence quantum efficiency of nanocrystalline ZnS:Mn^{2+}. 1. Surface passivation and Mn^{2+} concentration, J. Phys. Chem. B 105 (2001) 10197–10202.